

ARTICLE

Received 11 Sep 2014 | Accepted 27 Jul 2015 | Published 8 Sep 2015

DOI: 10.1038/ncomms9188

Anomalous quantum criticality in an itinerant ferromagnet

C.L. Huang^{1,2,†}, D. Fuchs¹, M. Wissinger¹, R. Schneider¹, M.C. Ling³, M.S. Scheurer³, J. Schmalian^{1,3}
& H.v. Löhneysen^{1,2}

The dynamics of continuous phase transitions is governed by the dynamic scaling exponent relating the correlation length and correlation time. For transitions at finite temperature, thermodynamic critical properties are independent of the dynamic scaling exponent. In contrast, at quantum phase transitions where the transition temperature becomes zero, static and dynamic properties are inherently entangled by virtue of the uncertainty principle. Consequently, thermodynamic scaling equations explicitly contain the dynamic exponent. Here we report on thermodynamic measurements (as a function of temperature and magnetic field) for the itinerant ferromagnet $\text{Sr}_{1-x}\text{Ca}_x\text{RuO}_3$ where the transition temperature becomes zero for $x = 0.7$. We find dynamic scaling of the magnetization and specific heat with highly unusual quantum critical dynamics. We observe a small dynamic scaling exponent of 1.76 strongly deviating from current models of ferromagnetic quantum criticality and likely being governed by strong disorder in conjunction with strong electron–electron coupling.

¹Institut für Festkörperphysik, Karlsruher Institut für Technologie, 76021 Karlsruhe, Germany. ²Physikalisches Institut, Karlsruher Institut für Technologie, 76128 Karlsruhe, Germany. ³Institut für Theorie der Kondensierten Materie, Karlsruher Institut für Technologie, 76128 Karlsruhe, Germany. † Present address: Max Planck Institute for Chemical Physics of Solids, 01187 Dresden, Germany. Correspondence and requests for materials should be addressed to C.L.H. (email: clhuang1980@gmail.com) or to J.S. (email: joerg.schmalian@kit.edu) or to H.L. (email: hilbert.loehneysen@kit.edu).

SrRuO₃ is a three-dimensional itinerant ferromagnet with the Curie temperature $T_C \approx 160$ – 165 K (refs 1–4). It crystallizes in an orthorhombic perovskite structure with tilted RuO₆ octahedra. In the $4d^4$ configuration of Ru⁴⁺, the t_{2g} levels are occupied in a low-spin $S = 1$ state⁵. Ferromagnetism of SrRuO₃ can be suppressed by applying hydrostatic pressure, down to $T_C \approx 50$ K at a pressure of 17 GPa⁶. Alternatively, T_C is suppressed all the way to absolute zero on substitution of Sr²⁺ by the smaller Ca²⁺ ions at a critical concentration $x_c \approx 0.7$, where Sr_{1-x}Ca_xRuO₃ (SCRO) turns from a ferromagnetic (FM) to a paramagnetic ground state. Whether a quantum critical point (QCP) may be present at x_c is a matter of current debate^{2,4,7,8}. While specific heat³ and NMR⁴ measurements both concluded that the self-consistent renormalization theory⁹, equivalent to the Hertz–Millis model^{10,11}, could describe the underlying physics of an FM QCP in SCRO, recent Kerr effect measurements on a composition-spread epitaxial film showed that a possible quantum phase transition (QPT) around a (reduced) critical concentration x_c were smeared by disorder originating from the difference of ionic radii between Sr and Ca ions⁸. In addition, on the basis of muon-spin-rotation (μ SR) experiments, it was argued that a spontaneous phase separation may be a common feature in FM systems near their QPTs, leading to a suppression of dynamic critical behaviour^{7,12}. From the theoretical point of view, the conventional Hertz–Millis–Moriya model^{9–11} predicts, for three-dimensional itinerant magnets, dynamical critical exponents $z = 2$ for antiferromagnets, as well as $z = 3$ for clean and $z = 4$ for disordered ferromagnets¹⁰. While $z = 2$ has been observed in some antiferromagnets with spin-density-wave order¹³, there are important examples for deviations from the expectation for ferromagnets. Indeed, the model breaks down in the FM case,

because extra singular terms arising from fermionic modes, in addition to the order-parameter fluctuations, lead to multiple time scales^{14–16}. Moreover, in some composition-driven QPTs, close to the critical concentration x_c , disorder effects introduce additional fluctuations, giving rise to a nonanalytic contribution to the free energy between the paramagnetic and locally FM-ordered regions, known as the Griffiths rare regions^{17–19}.

In the following, we report on a consistent dynamical scaling analysis of the magnetization and specific heat for an $x = 0.7$ sample, bearing all features of a QCP with, however, very unusual critical exponents. In particular, we observe a small dynamic critical exponent $z = 1.76$, which strongly deviates from current models, and may arise from an inhomogeneous electron liquid due to the strong disorder induced by Ca substitution.

Results

Magnetic susceptibility and specific heat of Sr_{0.3}Ca_{0.7}RuO₃. As an overview, we show in Fig. 1a the magnetic d.c. susceptibility $\chi = M/B$, where M is the magnetization and B is the magnetic field, and its reciprocal value χ^{-1} versus temperature T for $1.8 \text{ K} \leq T \leq 50 \text{ K}$. While $\chi(T)$ increases with decreasing T down to the lowest temperature of 1.8 K, $\chi^{-1}(T)$ shows initially a downward curvature and levels off toward lower T . Notice the gradual change of $\chi^{-1}(T)$ from negative to positive curvature with decreasing temperature. The specific heat $C(T)$ of Sr_{0.3}Ca_{0.7}RuO₃ is shown in Fig. 1b in a plot of C/T versus T^2 . Between 20 and 30 K, the specific heat can be described by $C/T = \gamma_h + \beta_{ph}T^2$, where the subscript ‘h’ denotes the extrapolation of C/T from high temperatures to $T = 0$ and $\beta_{ph}T^3$ is the usual low- T Debye phonon contribution (see solid line in Fig. 1b). Below ≈ 15 K, a positive deviation of C/T from the C/T versus T^2 line is observed with a maximum of C/T for $T \rightarrow 0$, that is, a zero-temperature cusp. This deviation has been found before and was attributed to spin fluctuations of Ru⁴⁺ moments³. However, FM fluctuations should lead to a divergence of C/T at x_c for $T \rightarrow 0$, for example, $C/T \sim \log(T_0/T)$. This is not observed in Sr_{0.3}Ca_{0.7}RuO₃ as will be discussed in more detail below.

Figure 2a shows that the magnetic susceptibility $\chi(T)$ increases more slowly from $T = 30$ to 1.8 K in weak fields. The divergence of $\chi(T)$ continuously weakens towards lower T , and is increasingly suppressed already in weak magnetic fields. Figure 2b shows that, correspondingly, the magnetic isotherms $M(B)$ increase less rapidly with increasing T . The smooth curvatures of $\chi(T, B)$ and $M(T, B)$ suggest the applicability of a scaling relation. We therefore assume that the $x = 0.7$ sample is close to a QCP, see inset of Fig. 1b, as will be substantiated below.

Quantum critical scaling of thermodynamic properties. At a QCP with hyperscaling, that is, below the upper critical dimension, the scaling relation for the critical part of the free energy $\mathcal{F}(T, B)$ reads

$$\mathcal{F}(T, B) = b^{-(d+z)} \mathcal{F}(b^z T, b^{\beta\delta/\nu} B), \quad (1)$$

where b is an arbitrary scale factor and z and $\beta\delta/\nu$ are scaling exponents associated with the tuning parameters T and B , respectively. As usual, ν is the correlation length exponent that can be obtained from an analogous scaling relation involving the distance $r = x_c - x$ from the critical concentration ($\xi \propto |r|^{-\nu}$). δ and β describe the field and concentration dependence of the order-parameter $M(r = 0, T = 0, B) \propto B^{1/\delta}$ and $M(r, T = 0, B = 0) \propto r^\beta$, respectively. For the field and temperature dependence of the magnetization M follows:

$$M(T, B) = - \frac{\partial \mathcal{F}}{\partial B} = b^{\beta\delta/\nu - (d+z)} M(b^z T, b^{\beta\delta/\nu} B). \quad (2)$$

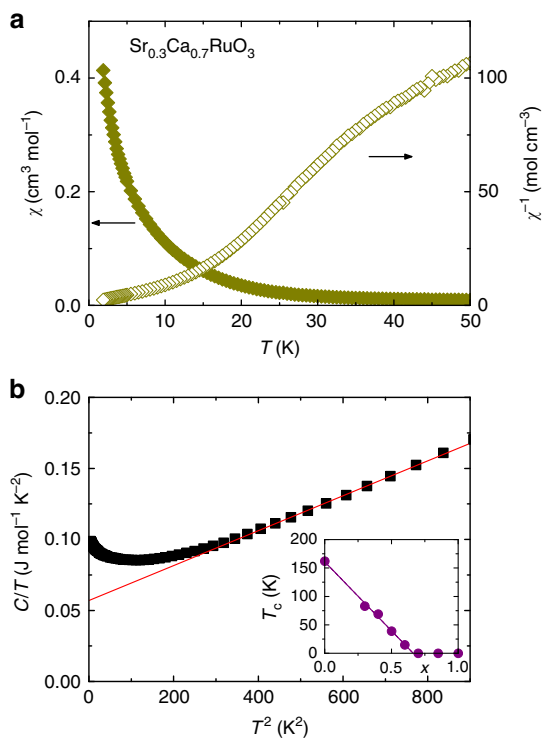


Figure 1 | Low-temperature magnetic susceptibility χ and specific heat C for Sr_{0.3}Ca_{0.7}RuO₃. (a) Left axis shows χ and right axis shows χ^{-1} . The data were measured in the field-cooled mode at $B = 10$ mT. (b) Zero-field C/T versus T^2 . The solid line represents the fit of $C/T = \gamma_h + \beta_{ph}T^2$ between $T = 20$ and 30 K with $\gamma_h = 0.064 \text{ J mol}^{-1} \text{ K}^{-2}$ and $\beta_{ph} = 1.3 \times 10^{-4} \text{ J mol}^{-1} \text{ K}^{-4}$. The inset shows T_C as a function of Ca concentration x (ref. 21).

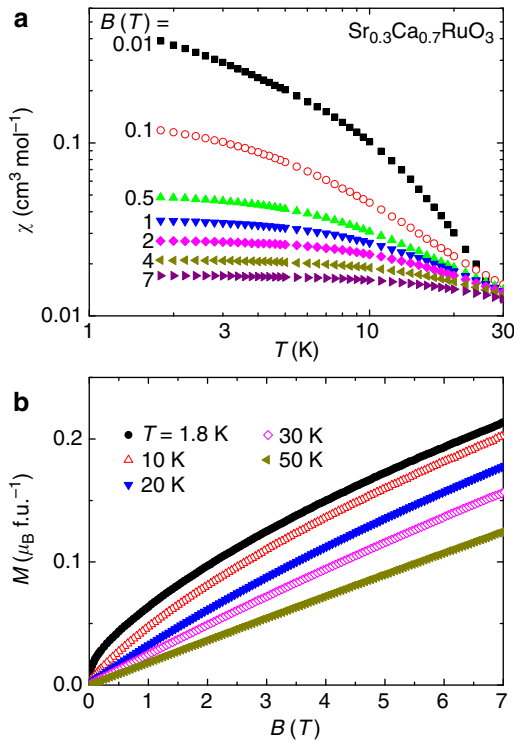


Figure 2 | Magnetic susceptibility χ and magnetization M of $\text{Sr}_{0.3}\text{Ca}_{0.7}\text{RuO}_3$. (a) Field-cooled χ versus temperature T measured at several different magnetic fields. (b) Magnetic isotherms measured at several different temperatures. Data are shown in part only for clarity.

With the choice of $b^z T = T_0$ with the cutoff energy $k_B T_0$, we get

$$M(T, B) = T^{\beta/vz} \Phi\left(B/T^{\beta\delta/vz}\right). \quad (3)$$

Hence, $M/T^{\beta/vz}$ should be a function of $B/T^{\beta\delta/vz}$. Our data obey the scaling behaviour (Equation (3)). As discussed in the Supplementary Note 1, the smallest error bars occur when the ratio of the two exponents β/vz and $\beta\delta/vz$ is close to 1.6. This determines the exponent $\delta \approx 1.6$ in good agreement with a previous estimate by Itoh *et al.*²⁰ To determine the other exponents, we first resort to quantum critical scaling properties of the specific heat that allows an unequivocal determination of d/z and $\beta\delta/vz$. Then we will return to a discussion of the magnetization data.

The scaling behaviour of the critical part of the specific heat is given by

$$C_{cr}(T, B) = -T \frac{\partial^2 \mathcal{F}}{\partial T^2} = b^{-d} C_{cr}\left(b^z T, b^{\beta\delta/vz} B\right). \quad (4)$$

Putting again $b^z T = T_0$ yields

$$C_{cr}(T, B) = T^{d/z} \Psi\left(B/T^{\beta\delta/vz}\right). \quad (5)$$

As long as $d > z$, this critical contribution at zero field is subleading to the quasiparticle contribution to the specific heat. Nevertheless, equation (5) allows an unequivocal determination of d/z from the zero-field-specific heat, that is, $C_{cr}(T, 0) = T^{d/z} \Psi(0)$.

Figure 3 shows that $\Delta C/T = C/T - \beta_{ph} T^2$ (with the phonon contribution subtracted) is well described by $\Delta C/T = \gamma_0 - aT^{0.7}$ with $\gamma_0 = 106 \text{ mJ mol}^{-1} \text{ K}^{-2}$ and $a = 6.0 \text{ mJ mol}^{-1} \text{ K}^{2.7}$ between 1.8 K up to 13 K. Hence, the subleading contribution $C_{cr}/T \propto T^{0.7}$ to the specific heat is clearly visible in the zero-field data. The inset of Fig. 3 displays the root-mean square (r.m.s.) deviation $\chi_{r.m.s.}$ versus $d/z - 1$ yielding $d/z - 1 = 0.70 \pm 0.04$ (see

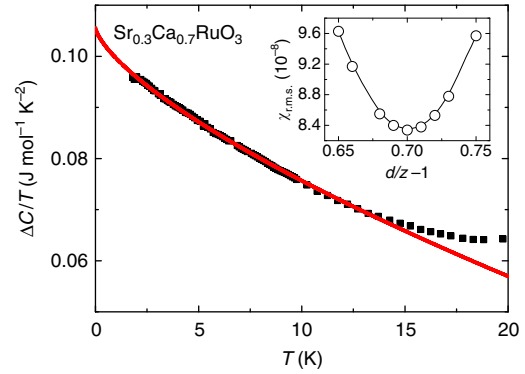


Figure 3 | Zero-field-specific heat ΔC of $\text{Sr}_{0.3}\text{Ca}_{0.7}\text{RuO}_3$. The phonon contribution has been subtracted. The solid line represents a fit of $\Delta C/T = \gamma_0 - aT^{0.7}$ between 1.8 and 13 K. The inset shows how the quality of the fit varies with $(d - z)/z$ in equation (5) by checking the smallest mean square deviation $\chi_{r.m.s.}$.

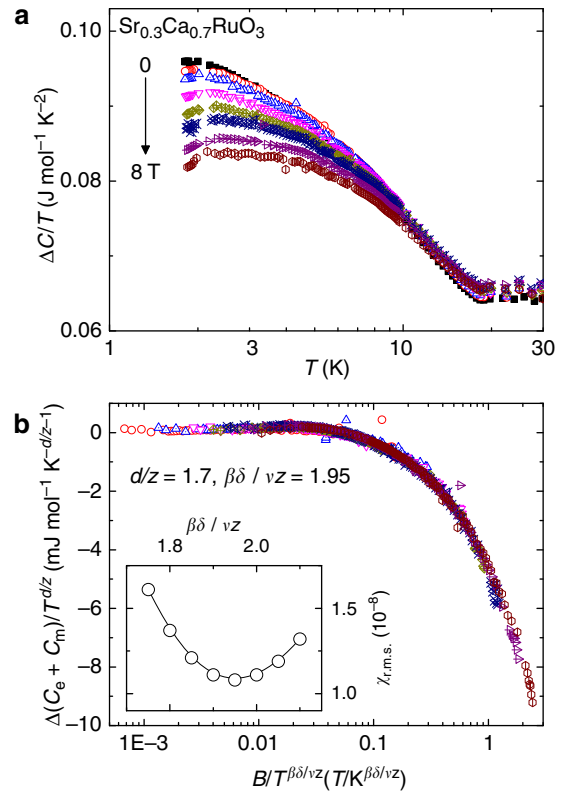


Figure 4 | Critical contribution to the specific heat C . (a) ΔC (phonon contribution subtracted) of $\text{Sr}_{0.3}\text{Ca}_{0.7}\text{RuO}_3$ plotted as $\Delta C/T$ versus $\log T$ at fields $B = 0, 0.5, 1, 2, 3, 4, 6$ and 8 T from top to the bottom. (b) Scaling of the field-dependent specific heat data from (a). The inset shows how the quality of the scaling collapse varies with $\beta\delta/vz$ (with fixed value $d/z = 1.7$) by checking the smallest mean square deviation $\chi_{r.m.s.}$.

Supplementary Fig. 1). The striking result following immediately is that the dynamic critical exponent for $d = 3$ is $z = 1.76 \pm 0.04$.

Turning to the field dependence of the specific heat, Fig. 4a shows $C(T, B)$ plotted as $\Delta C/T$ versus $\log T$. With increasing field, the cusp of C/T for $T \rightarrow 0$ (see Fig. 3) becomes rounded and, for $B \geq 1 \text{ T}$, $\Delta C/T$ even falls off slightly towards the lowest measuring temperature. The gradual decrease of $\Delta C/T$ from $B = 0$ to 8 T amounts to only 15% in this T range. To check for QCP

temperature-field scaling of the specific heat, we plot $(C(T, B) - C(T, 0))/T^{d/z}$ versus $B/T^{\beta\delta/vz}$ in Fig. 4b. The zero-field contribution is subtracted to eliminate the non-critical quasiparticle contribution to C . With $d/z = 1.70$ as determined above, we find very good scaling over more than three orders of magnitude in $B/T^{\beta\delta/vz}$ with $\beta\delta/vz = 1.95 \pm 0.1$ (Supplementary Fig. 1). The inset of Fig. 4b shows a plot of $\chi_{r.m.s.}$ versus the fitting exponent $\beta\delta/vz$. Due to the small critical contribution to C , the scatter of the scaling plot is somewhat larger.

Critical scaling of the susceptibility and magnetization. We are now in the position to obtain the quantum critical scaling plots for the susceptibility and magnetization data. Figure 5a,b shows the corresponding plots obtained, respectively, from the $\chi(T, B)$ data of Fig. 2a measured as a function of T for different fields and from the $M(T, B)$ data of Fig. 2b measured as a function of B for different temperatures. Here we have omitted the data of very low fields ($B \leq 0.1$ T of Fig. 2a) where scaling is not expected because of domain effects. Very good scaling over more than three orders of magnitude of $B/T^{\beta\delta/vz}$ is found for both data sets with $\beta/vz = 1.2 \pm 0.05$ using $\beta\delta/vz = 1.95$ determined from the specific heat (Supplementary Fig. 2 and Fig. 3). Again, the determination of β/vz is corroborated by $\chi_{r.m.s.}$ minima shown in the plots of Fig. 5a,b. Our result for β/vz slightly larger than unity is consistent with the experimental observation that $T_C(r) \propto r^{vz}$ is roughly proportional to the low- T magnetization $\propto r^\beta$ (ref. 21). The comparatively small value $\delta = 1.63 \pm 0.15$ that emerges embodies the soft divergence of the susceptibility mentioned earlier. Remember that $\delta = 3$ is the mean-field value for the exponent, a value that is usually enhanced via critical fluctuations. Hence, the anomalously small dynamic exponent z obtained from the specific heat results is accompanied by an equally unusual

small exponent δ . Using the usual scaling laws, our results further imply a rather large value of the exponent $\eta \approx 0.73$ that determines the spatial/momentum variation of the susceptibility $\chi(q) \propto q^{-(2-\eta)}$ and gives evidence for highly non-local quantum fluctuations.

Discussion

The consistent dynamic scaling analysis of magnetization and specific heat of SCRO at the QCP $x_c = 0.7$ raises questions to the origin of this highly unusual behaviour. The very observation of scaling of the susceptibility suggests that we are below the upper critical dimension. Together with the numerical value for z , this fact implies that the universality class of the transition cannot be of the conventional ϕ^4 type, where $d+z > 4$ would place the system in the mean-field regime. In addition, the negative sign of the critical contribution suggests that one cannot interpret $C_{cr}(T)$ as specific heat of isolated collective degrees of freedom but, rather, that the critical dynamics is intertwined with the dynamics of quasiparticles. One possible interpretation is clearly related to the emergence of inhomogeneities. Scale-dependent strain fields, caused by the different values of the ionic radii of Sr and Ca can lead to modified effective exponents²². The μ SR relaxation rate T_1^{-1} of SCRO for $x = 0.7$ was found to exhibit at low T a behaviour $T_1 \sim \text{constant}$ ¹². A scaling analysis leads to $T_1 \propto T^\theta$ with $\theta z = (\delta - 1)\beta/v - d$, which for our data yields $\theta \cong -1$. Given this finding it is important to further experimentally investigate T_1 in the low-temperature regime.

The key observation of this paper are the small values of the exponents δ and z , if compared with the mean-field Hertz–Moriya–Millis theory¹⁰ for clean ($\delta = 3, z = 3$) or weakly disordered ($\delta = 3, z = 4$) systems. Important deviations from mean-field behaviour, based on nonanalytic corrections to Fermi-liquid theory²³, have been investigated in the vicinity of a ferromagnetic critical point and yield weak first-order transitions^{23–25}, instead of fundamentally new critical exponents that are found experimentally in SCRO. Different values for critical exponents have in fact been discussed as a result of the vicinity to a quantum tricritical point²⁶ or due to preasymptotic critical behaviour in disordered systems²⁷. Both approaches yield values for δ rather close to our findings. However, the substantially different value of the dynamical critical exponent found here cannot be explained in refs 26,27.

The small value of z seems, however, consistent with a strong-coupling perspective of the coupling between collective magnetic degrees of freedom and incoherent quasiparticle excitations. Away from the critical point, it was shown^{28,29} that the appropriate description of metallic quantum ferromagnets is in terms of quasiparticles that interact with the coherent magnetization motion via an abelian gauge field. For such a gauge coupling between critical degrees of freedom and the quasiparticle excitations, one would naturally expect a reduced value of the quasiparticle damping and, thus, of the dynamic critical exponent z . Naively, this is due to the fact that in the strong-coupling regime the magnitude of the magnetization is expected to be large even at the QCP, while long-range order is destroyed via directional fluctuations. Hence, the coupling to the Stoner continuum is suppressed by the large magnitude of magnetization, similar to what happens in the ordered state. Our measurement strongly suggests to extend this strong-coupling description of quantum ferromagnetism all the way to the QCP. Regardless of the details, the very observation of dynamic scaling is strong evidence for a second-order transition settling an ongoing debate of this issue⁷. Further work should lead to a detailed understanding of the anomalously low dynamic critical exponent.

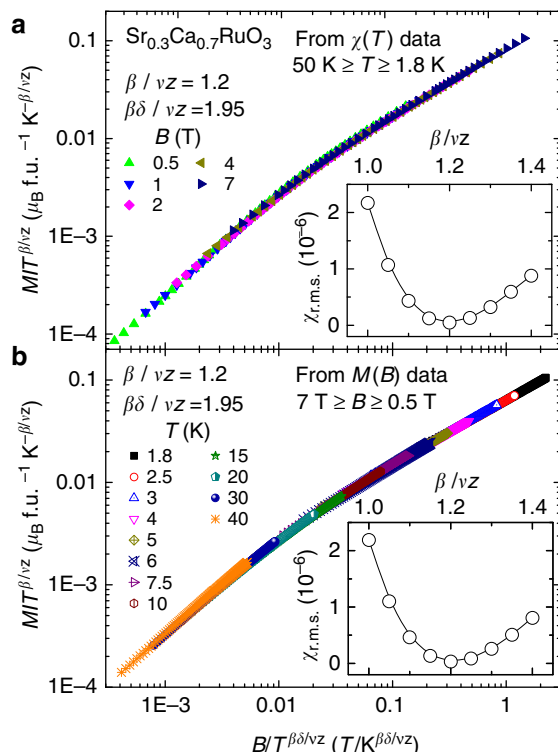


Figure 5 | Scaling of the magnetic susceptibility χ and magnetization M as a function of temperature T and magnetic field B . (a) Data from Fig. 2a. (b) Data from Fig. 2b. Insets show how the quality of the scaling collapse varies with β/vz (with fixed value $\beta\delta/vz = 1.95$) by checking the smallest mean square deviation $\chi_{r.m.s.}$.

Methods

Sample synthesis and experiments. The SCRO polycrystals were prepared by solid-state sintering using SrCO₃, CaCO₃ and RuO₂ powders as described in ref. 21. From the structural refinement of powder X-ray diffraction spectra, electron dispersive X-ray spectroscopy and wavelength dispersive X-ray spectroscopy, a stoichiometric single phase (space group *Pbnm*) was confirmed. The magnetization *M* and the specific heat *C* were measured in the temperature range *T* = 1.8–300 K and in magnetic fields up to *B* = 8 T. We used the same pieces of plate-like samples, with a typical size of 2 × 2 × 1 mm³, oriented parallel to the applied field in both measurements. The use of polycrystalline samples does not affect the possibility to reliably determine scaling exponents of phase transitions²¹, yet the concentration dependence of the critical exponents near the classical, finite-*T* transition is consistent with strain-induced anomalous scaling discussed in ref. 22, hinting at the role of inhomogeneities.

Determination of the critical concentration. Since one might wonder whether different values of critical concentration, that is, *x*_c ≠ 0.7, might lead to a different conclusion on anomalously small dynamic scaling exponent, we further discuss this issue in detail in Supplementary Note 2. From Supplementary Fig. 4, *x*_c may be accurate within 3% only. To check the ramifications of this uncertainty, we have additionally carried out a scaling analysis of a sample with *x* = 0.75 (Supplementary Figs 5 and 6). This analysis suggests that while the critical exponents vary slightly when assuming *x*_c = 0.75, they are still highly anomalous compared with those of the conventional Hertz–Millis–Moriya model. Using this variation, we show that even if the critical concentration was *x* = 0.65, this would still give anomalous exponents.

References

- Longo, J. M., Raccach, P. M. & Goodenough, J. B. Magnetic properties of SrRuO₃ and CaRuO₃. *J. Appl. Phys.* **39**, 1327–1328 (1968).
- Cao, G., McCall, S., Shepard, M., Crow, J. E. & Guertin, R. P. Thermal, magnetic, and transport properties of single-crystal Sr_{1-x}Ca_xRuO₃ (0 < *x* < 1.0). *Phys. Rev. B* **56**, 321–329 (1997).
- Kiyama, T., Yoshimura, K., Kosuge, K., Michor, H. & Hilscher, G. Specific heat of (Sr-Ca)RuO₃. *J. Phys. Soc. Jpn* **67**, 307–311 (1998).
- Yoshimura, K. *et al.* ¹⁷O NMR observation of universal behavior of ferromagnetic spin fluctuations in the itinerant magnetic system Sr_{1-x}Ca_xRuO₃. *Phys. Rev. Lett.* **83**, 4397–4400 (1999).
- Mazin, I. I. & Singh, D. J. Electronic structure and magnetism in Ru-based perovskites. *Phys. Rev. B* **56**, 2556–2571 (1997).
- Hamlin, J. J. *et al.* ac susceptibility studies of the weak itinerant ferromagnet SrRuO₃ under high pressure to 34 GPa. *Phys. Rev. B* **76**, 014432 (2007).
- Uemura, Y. J. *et al.* Phase separation and suppression of critical dynamics at quantum phase transitions of MnSi and (Sr_{1-x}Ca_x)RuO₃. *Nat. Phys.* **3**, 29–35 (2007).
- Demkó, L. *et al.* Disorder promotes ferromagnetism: Rounding of the quantum phase transition in Sr_{1-x}Ca_xRuO₃. *Phys. Rev. Lett.* **108**, 185701 (2012).
- Konno, R. & Moriya, T. Quantitative aspects of the theory of nearly ferromagnetic metals. *J. Phys. Soc. Jpn* **56**, 3270–3278 (1987).
- Hertz, J. A. Quantum critical phenomena. *Phys. Rev. B* **14**, 1165–1184 (1976).
- Millis, A. J. Effect of a nonzero temperature on quantum critical points in itinerant fermion systems. *Phys. Rev. B* **48**, 7183–7196 (1993).
- Gat-Malureanu, I. M. *et al.* Muon spin relaxation and susceptibility measurements of an itinerant-electron system Sr_{1-x}Ca_xRuO₃: quantum evolution from ferromagnet to paramagnet. *Phys. Rev. B* **84**, 224415 (2011).
- Zhu, L., Garst, M., Rosch, A. & Si, Q. Universally diverging Grüneisen parameter and the magnetocaloric effect close to quantum critical points. *Phys. Rev. Lett.* **91**, 066404 (2003).
- Belitz, D., Kirkpatrick, T. R. & Vojta, T. How generic scale invariance influences quantum and classical phase transitions. *Rev. Mod. Phys.* **77**, 579–632 (2005).
- Löhneysen, H. v., Rosch, A., Vojta, M. & Wölfle, P. Fermi-liquid instabilities at magnetic quantum phase transitions. *Rev. Mod. Phys.* **79**, 1015–1075 (2007).
- Belitz, D., Kirkpatrick, T. R. & Rollbühler, J. Tricritical behavior in itinerant quantum ferromagnets. *Phys. Rev. Lett.* **94**, 247205 (2005).
- Vojta, T. Rare region effects at classical, quantum and nonequilibrium phase transitions. *J. Phys. A* **39**, R143–R205 (2006).
- Vojta, T. Quantum Griffiths effects and smeared phase transitions in metals: Theory and experiment. *J. Low. Temp. Phys.* **161**, 299–323 (2010).
- Ubaid-Kassis, S., Vojta, T. & Schroeder, A. Quantum Griffiths phase in the weak itinerant ferromagnetic alloy Ni_{1-x}V_x. *Phys. Rev. Lett.* **104**, 066402 (2010).
- Itoh, Y., Mizoguchi, T. & Yoshimura, K. Novel critical exponent of magnetization curves near the ferromagnetic quantum phase transitions of Sr_{1-x}A_xRuO₃ (A = Ca, La_{0.5}Na_{0.5}, and La). *J. Phys. Soc. Jpn* **77**, 123702 (2008).
- Fuchs, D. *et al.* Critical scaling analysis of the itinerant ferromagnet Sr_{1-x}Ca_xRuO₃. *Phys. Rev. B* **89**, 174405 (2014).
- Belitz, D., Kirkpatrick, T. R. & Saha, R. Criticality in inhomogeneous magnetic systems: Application to quantum ferromagnets. *Phys. Rev. Lett.* **99**, 147203 (2007).
- Belitz, D., Kirkpatrick, T. R. & Vojta, T. Nonanalytic behavior of the spin susceptibility in clean Fermi systems. *Phys. Rev. B* **55**, 9452–9462 (1997).
- Rech, J., Pepin, C. & Chubukov, A. Quantum critical behavior in itinerant electron systems: Eliashberg theory and instability of a ferromagnetic quantum critical point. *Phys. Rev. B* **74**, 195126 (2006).
- Conduit, G. J., Green, A. G. & Simons, B. D. Inhomogeneous phase formation on the border of itinerant ferromagnetism. *Phys. Rev. Lett.* **103**, 207201 (2009).
- Misawa, T., Yamaji, Y. & Imada, T. YbRh₂Si₂: Quantum Tricritical Behavior in Itinerant Electron Systems. *J. Phys. Soc. Jpn* **77**, 093712 (2008).
- Kirkpatrick, T. R. & Belitz, D. Preasymptotic critical behavior and effective exponents in disordered metallic quantum ferromagnets. *Phys. Rev. Lett.* **113**, 127203 (2014).
- Korenman, V., Murray, J. L. & Prange, R. E. Local-band theory of itinerant ferromagnetism. I. Fermi-liquid theory. *Phys. Rev. B* **16**, 4032–4047 (1977).
- Volovik, G. E. Linear momentum in ferromagnets. *J. Phys. C Solid State Phys.* **20**, L83–L87 (1987).

Acknowledgements

This work was supported by the Deutsche Forschungsgemeinschaft through the Research Unit FOR 960. We thank J. L. Her, K. Yoshimura, C. Meingast and R. Heid for helpful discussions.

Author contributions

C.L.H. set up and carried out the magnetization and specific heat measurements. C.L.H., D.F. and H.v.L. discussed the experimental data. D.F., M.W. and R.S. synthesized and characterized the samples. M.C.L., M.S.S. and J.S. performed the dynamic scaling analysis. H.v.L. planned and headed the project. C.L.H., J.S. and H.v.L. wrote the paper.

Additional information

Supplementary Information accompanies this paper at <http://www.nature.com/naturecommunications>

Competing financial interests: The authors declare no competing financial interests.

Reprints and permission information is available online at <http://npng.nature.com/reprintsandpermissions/>

How to cite this article: Huang, C. L. *et al.* Anomalous quantum criticality in an itinerant ferromagnet. *Nat. Commun.* 6:8188 doi: 10.1038/ncomms9188 (2015).